Received: 15 February 2021 | Revised: 5 July 2021 | Accepted: 19 July 2021

DOI: 10.1096/fj.202100276RR

THE FASEB JOURNAL

RESEARCH ARTICLE

Transcriptomic links to muscle mass loss and declines in cumulative muscle protein synthesis during short-term disuse in healthy younger humans

Craig R. G. Willis[1] | **Iain J. Gallagher**[2] | **Daniel J. Wilkinson**[3] | **Matthew S. Brook**[3] | **Joseph J. Bass**[3] | **Bethan E. Phillips**[3] | **Kenneth Smith**[3] | **Timothy Etheridge**[1] | **Tanner Stokes**[4] | **Chris McGlory**[4] | **Stefan H. M. Gorissen**[4] | **Nathaniel J. Szewczyk**[3,5] | **Stuart M. Phillips**[4] | **Philip J. Atherton**[3]

[1]Department of Sport and Health Sciences, College of Life and Environmental Sciences, University of Exeter, Exeter, UK

[2]Faculty of Health Sciences and Sport, University of Stirling, Stirling, UK

[3]MRC-Versus Arthritis Centre for Musculoskeletal Ageing Research and National Institute of Health Research, Nottingham Biomedical Research Centre, Royal Derby Hospital Centre, School of Medicine, University of Nottingham, Derby, UK

[4]Department of Kinesiology, McMaster University, Hamilton, ON, Canada

[5]Ohio Musculoskeletal and Neurological Institute (OMNI) and Department of Biomedical Sciences, Ohio University, Athens, OH, USA

Correspondence
Philip J. Atherton, MRC-Versus Arthritis Centre for Musculoskeletal Ageing Research and National Institute of Health Research, Nottingham Biomedical Research Centre, Royal Derby Hospital Centre, School of Medicine, University of Nottingham, Derby, DE22 3DT, UK.
Email: philip.atherton@nottingham.ac.uk

Funding information
RCUK | Biotechnology and Biological Sciences Research Council (BBSRC), Grant/Award Number: BB/J014400/1, BB/M009122/1 and BB/N015894/1; Gouvernement du Canada | Natural Sciences and Engineering Research Council of Canada (NSERC); RCUK | Medical Research Council (MRC), Grant/Award Number: MR/P021220/1 and MR/R502364/1

Abstract

Muscle disuse leads to a rapid decline in muscle mass, with reduced muscle protein synthesis (MPS) considered the primary physiological mechanism. Here, we employed a systems biology approach to uncover molecular networks and key molecular candidates that *quantitatively link* to the degree of muscle atrophy and/or extent of decline in MPS during short-term disuse in humans. After consuming a bolus dose of deuterium oxide (D_2O; 3 $mL.kg^{-1}$), eight healthy males (22 ± 2 years) underwent 4 days of unilateral lower-limb immobilization. Bilateral muscle biopsies were obtained post-intervention for RNA sequencing and D_2O-derived measurement of MPS, with thigh lean mass quantified using dual-energy X-ray absorptiometry. Application of weighted gene co-expression network analysis identified 15 distinct gene clusters ("modules") with an expression profile regulated by disuse and/or quantitatively connected to disuse-induced muscle mass or MPS changes. Module scans for candidate targets established an experimentally tractable set of candidate regulatory molecules (242 hub genes, 31

Abbreviations: BP, biological process; CC, cellular component; D_2O, deuterium oxide; DXA, dual-energy X-ray absorptiometry; ECM, extracellular matrix; FDR, false discovery rate; GO, Gene Ontology; GS, gene significance; kIM, within-module connectivity; MF, molecular function; MPB, muscle protein breakdown; MPS, muscle protein synthesis; mTORC1/2, mTOR complexes 1 and 2; TFBS, transcription factor binding site(s); ULLI, unilateral lower-limb immobilization; WGCNA, weighted gene co-expression network analysis.

Craig R. G. Willis and Iain J. Gallagher are co-first authors.

transcriptional regulators) associated with disuse-induced maladaptation, many themselves potently tied to disuse-induced reductions in muscle mass and/or MPS and, therefore, strong *physiologically relevant* candidates. Notably, we implicate a putative role for muscle protein breakdown-related molecular networks in impairing MPS during short-term disuse, and further establish DEPTOR (a potent mTOR inhibitor) as a critical mechanistic candidate of disuse driven MPS suppression in humans. Overall, these findings offer a strong benchmark for accelerating mechanistic understanding of short-term muscle disuse atrophy that may help expedite development of therapeutic interventions.

KEYWORDS

atrophy, disuse, gene network analysis, muscle protein synthesis, skeletal muscle

1 | INTRODUCTION

Reduced physical activity occurring during injury, illness, spaceflight, or with certain lifestyle choices, results in muscle disuse. Even in healthy people, muscle disuse leads to muscle atrophy,[1,2] the health consequences of which include reduced strength and endurance,[3] impaired insulin sensitivity,[4] and reduced anabolic responsiveness to protein intake.[5] Temporally, muscle disuse atrophy is a rapidly occurring phenomenon, with the rate of muscle loss being most pronounced during the initial stages (ie, ≤7 days) of disuse.[6,7] This has significant clinical bearing, not only since the typical length of hospital stay or home-based inactivity following illness/injury is ≤1 week,[7-11] but also because the aggregation of such short periods of disuse throughout life accelerates age-related muscle loss (ie, "sarcopenia").[6] With acute hospital admissions and the aging population expanding,[12,13] the contribution of short-term muscle disuse to muscle dysfunction is of increasing concern. Muscle disuse atrophy is a phenomenon intrinsic to the affected muscle(s) (thus termed "simple" atrophy),[14,15] yet there are often comorbidities present that may contribute further to atrophy, such as whole-body insulin resistance[16] or systemic inflammation[17] as seen in aging[18] or metabolic disease.[19]

The most frequently used models for studying muscle disuse atrophy in humans are bed rest, and unilateral lower-limb immobilization (ULLI; as with musculoskeletal rehabilitation) via, for example, bracing/casting or limb suspension.[6] Although bed rest is arguably more clinically relevant, whether it is an appropriate mechanistic model to study disuse atrophy has been debated.[1,20,21] Indeed, systemic influences arising during bed rest (eg, systemic inflammation, hormonal alterations) make it difficult to isolate the intrinsic mechanisms driving disuse atrophy.[1,20] In contrast, this issue is moderated with ULLI, since disuse remains isolated to a single limb or muscle group. Such a model also permits use of the contralateral leg as a co-temporal control, enabling a more robust physiologic/molecular signal to be obtained within individuals. As a consequence, ULLI can be considered a highly appropriate experimental model to better understand the mechanisms driving short-term disuse atrophy per se.[1]

Muscle mass is maintained through a dynamic balance between muscle protein synthesis (MPS) and muscle protein breakdown (MPB).[22] Disuse atrophy must, therefore, be underpinned by net imbalance between the two. MPS (both fed and fasted) has been shown to decline with short-term immobilization (5 days) in younger, healthy individuals,[5] while there remains a lack of direct evidence for any quantifiable change in MPB in humans.[14,15] On this basis, attenuated MPS is considered the predominant physiological mechanism of (non-diseased) short-term disuse atrophy[23] and hence a primary target for therapeutic intervention.[23,24] A critical limiting factor in this regard, however, is that the molecular regulation of MPS remains poorly understood in the context of short-term disuse. Indeed, of the few benchmark molecular investigations that exist to date (ie, those utilizing ULLI in younger, healthy cohorts), most remain as targeted analysis of "established" MPS markers (eg, Akt/mTOR), with either a lack of direct relation to, or inclusion of, measures of MPS/muscle mass across most previous research efforts: hindering the ability for one to draw more robust conclusions on molecular causality.[5,25-30] In any case, the molecular complexity of muscle is overlooked by viewing molecular changes as isolated events, as is the case for targeted molecular profiling or transcriptome-wide gene-level differential expression efforts that have been undertaken to date.[5,25-30] Further worthy of consideration is that, while muscle mass and MPS do indeed decline as a result of disuse, there also appears to exist notable inter-individual variability in muscle physiologic responses to unloading,[7,26,31] implying that molecular regulation of muscle disuse is too somewhat heterogeneous. Accounting for such molecular/physiological heterogeneity consequently helps identify molecules that

regulate human muscle phenotypic adaptation.[32-34] Studies employing more untargeted approaches that both take into account the molecular complexity of muscle *and* facilitate linkage between molecular, MPS, and muscle mass changes therefore remain necessary before a complete blueprint of the intrinsic mechanisms regulating short-term human disuse atrophy can be attained.

Recently, we confirmed the efficacy of deuterium oxide (D_2O; "heavy water") techniques for quantification of MPS in free-living conditions over extended durations (ie, days-to-weeks).[35-37] This approach permits measurement of MPS over an entire period of disuse, providing valuable data to determine the mechanistic underpinnings of disuse atrophy.[26] More recently, we have demonstrated the power of network analysis as an advanced bioinformatic tool to uncover novel pathways and molecular drivers of human muscle (un)loading phenotypes.[34,38] As a systems biology concept, network analysis enables for the molecular complexity of a system to first be encapsulated by modeling interactions between its molecular components, with downstream network-driven analyses thereafter facilitating the discovery process of new, physiologically relevant molecules by providing an optimal basis to make direct connections between molecular responses and endpoint physiological changes.[39] Network analysis thus offers a judicious strategy to probe for novel molecular correlates of the short-term muscle disuse phenotype. Using data obtained as part of a new clinical study of healthy younger volunteers, we herein combined the above-mentioned bioinformatic and metabolic techniques with robust measures of muscle mass to establish key molecules *quantitatively linked* to the degree of muscle atrophy and/or extent of MPS suppression following 4 days of ULLI—in turn providing new insights into possible intrinsic mechanisms of short-term disuse atrophy in humans.

2 | MATERIALS AND METHODS

2.1 | Subject characteristics

Eight young, healthy male volunteers (mean ± SD: age, 22 ± 2 years; body mass index, 25 ± 3 $kg.m^{-2}$) were involved in this study. Volunteers were initially screened by medical questionnaire, with exclusions for history of any neuromuscular disorder or muscle/bone wasting disease, acute or chronic metabolic, respiratory or cardiovascular disorder, or any other signs of ill health. All subjects were recreationally active upon entry into the study, but were not routinely undertaking heavy, structured exercise. Subjects did not use tobacco-containing products or consume excessive alcohol (>21 units per week). The experimental procedures outlined herein were approved by the Hamilton Integrated Research Ethics Board (HiREB #2192) as part of a wider clinical trial registered at trialregister.nl (NTR6099) and conformed to the Declaration of Helsinki. Written informed consent was obtained from all subjects prior to their participation.

2.2 | Overview of experimental procedures

This study involved a bilateral leg protocol, with one leg randomly assigned to be immobilized and the other consequently used as a co-temporal contralateral control. Upon inclusion, subjects were asked to visit the laboratory on two separate occasions, both of which followed an overnight fast. On the first visit, participants had the thigh lean mass of both legs measured using dual-energy X-ray absorptiometry (DXA) (Lunar iDXA; GE Medical Systems, Mississauga, ON), before ingesting a bolus dose of D_2O (3 $mL.kg^{-1}$) for the measurement of integrated MPS rates. A saliva sample was obtained prior to and 2 hours following D_2O consumption for measurement of deuterium enrichment in body water. Thereafter, a knee brace (X-Act ROM; DonJoy, Dallas, TX, USA) was fitted to the immobilization leg and fixed at an angle of 60° of knee flexion. Participants wore the knee brace as described for a total duration of 4 full days, ambulating on crutches throughout the immobilization period and returning to the laboratory for their second visit exactly 4 days after their first visit. Upon arrival for visit 2, participants had their knee brace removed, the thigh lean mass of both legs again measured, and a further saliva sample was obtained. Finally, a skeletal muscle sample was collected from the *m. vastus lateralis* of each leg under local anesthesia using the Bergström needle technique,[40] with extracted tissue snap-frozen in liquid nitrogen and stored at −80°C until analysis.

2.3 | Quantification of thigh lean mass and MPS

DXA-derived thigh fat- and bone-free (ie, lean) mass (referred to herein as "muscle mass" for simplicity) was determined from the lowest point of the ischium to the knee space.[41] Myofibrillar MPS was quantified using the same protocol as is described in full elsewhere.[41] Post-intervention DXA data were unable to be obtained for one participant due to a technical issue, with all muscle mass-related analyses herein consequently based on data from seven of the eight participants. Physiologic data were analyzed via IBM SPSS (v26.0) using paired *t* test (MPS) or two-way repeated measures ANOVA with Fisher's LSD post-hoc analysis (muscle mass), with

data presented as mean ± SD and statistical significance set at $P < .05$.

2.4 | RNA-sequencing data generation

Muscle tissue (>30 mg per sample) was homogenized in Trizol reagent (Invitrogen) following the manufacturer's directions. After the addition of chloroform and subsequent centrifugation step the aqueous phase was transferred to RNeasy columns (Qiagen) for mRNA isolation following manufacturer directions. RNA was quantified using the Denovix DS11 FX+spectrophotometer (Denovix, UK). RNA quality was examined using the RNA iQ assay and the Qubit 4 instrument (Thermofisher, UK). All samples returned quality scores ≥8.1. Strand-specific mRNA libraries were prepared using the TruSeq Library Kit (Illumina, UK) and RNA sequenced to generate paired end reads using the NovaSeq 6000 instrument (Ilumina, UK) by Edinburgh Genomics, UK. All samples passed initial quality control. The RNA-sequenced reads were aligned to the human genome (version GrCH38, from Ensembl release 96) and summary counts generated using the R programming language and the Rsubread library.[42]

2.5 | Differential gene-level expression analysis

Differential gene expression analysis was undertaken using the R programming language and the edgeR library.[43] The count data were filtered using a counts-per-million bases threshold of 10 as recommended by the edgeR authors[44] and the filtered data normalized using the trimmed mean of M values algorithm as implemented in edgeR. To detect differential gene expression between the immobilized and non-immobilized legs we used a design matrix to account for the paired nature of the samples following guidance in the edgeR user's manual (Section 3.4—Additive models and blocking). Differential expression of genes was assessed with a likelihood ratio test using the glmLRT function of edgeR. The Benjamini-Hochberg procedure was used to control for false discovery rate (FDR). Genes with a Benjamini-Hochberg corrected P-value <.05 were defined as being differentially expressed.

2.6 | Co-expression network analysis: Network construction and module detection

A gene-wise network was constructed using the weighted gene co-expression network analysis (WGCNA) R library.[45] Before network construction, raw read counts of filtered genes were normalized using a variance-stabilizing transformation[46] in order to attain homoscedastic expression data. An adjacency matrix quantifying the connection strength between each pair of genes was then defined, in which entries equaled the 12th power of the Pearson's correlation coefficient between a given gene pair when the coefficient was positive, and zero otherwise. Such an adjacency structure is the basis for building a signed hybrid co-expression network—selected on the premise that signed variants appear more effective in identifying biologically coherent network modules than unsigned counterparts.[47] Moreover, the power of 12 was chosen following the scale-free topology criterion[48] and was the lowest exponent for which the corresponding scale-free topology fitting index metric (signed-R^2) achieved an appropriately high value (≥0.9). A relative interconnectedness measure for each gene pair (dissimilarity topological overlap) was then quantified from the adjacency matrix and subject to average linkage hierarchical clustering to generate a network tree, with network modules in turn determined using the *cutreeDynamic* algorithm.[49] Of note, a minimum module size of 50 genes was selected when defining modules, which were subsequently merged if their composite expression (module eigengene; first principal component of module gene expression) was very similar (correlation ≥ 0.75)—undertaken to obtain moderately large and distinct modules.[47,50] Modules were then assigned a unique numerical label "M*i*" for identification. Genes which could not be distinctly clustered were assigned to a module labeled "M0" and excluded from all subsequent analyses (but included in background gene lists where applicable).

2.7 | Co-expression network analysis: Defining disuse-associated modules

Molecular networks associated with short-term muscle disuse were characterized in two ways. First, molecular networks responsive to disuse were established by applying differential analysis (immobilization vs control) to the module eigengene. Such analysis was performed using empirical Bayes-moderated paired t tests as implemented in the limma package for R,[51] with differentially regulated modules selected as those with a Benjamini-Hochberg corrected P-value <.05. Second, module eigengene patterns were correlated with disuse-induced muscle mass (% loss, pre-to-post intervention of the immobilized leg) and MPS (% decrease, control vs immobilized leg) changes to elucidate molecular networks of possible physiologic relevance in the context of short-term disuse muscle adaptation. Physiologically relevant modules were subsequently defined as any network module for which the difference (Δ)

in eigengene expression between control and immobilized legs was significantly correlated ($|r| > 0.7$, $P < .05$) with a given physiologic variable.

2.8 | Ontological analysis of disuse-associated expression changes

The functional characteristics of differentially expressed genes and disuse-associated network modules were derived by testing the relevant gene lists for enrichment of Gene Ontology (GO) terms. Analyses was undertaken using the clusterProfiler package in R,[52] with the corresponding background gene list used in each instance being the genes used as input during differential expression testing/network construction. Each of the three separate GO categories (biological process, BP; cellular component, CC; and molecular function, MF) were considered during analyses, and enriched terms selected as those with a Benjamini-Hochberg corrected *P*-value <.05.

2.9 | Network-driven identification of key molecular drivers of disuse muscle adaptation

Primary candidate targets of disuse-induced human muscle adaptation were determined via two approaches. First, key molecular drivers within disuse-associated modules (module "hub" genes) were established as based on their scaled within-module connectivity (kIM),[53] such that genes within a given module with a scaled kIM value ≥ 0.7 were classified as module hubs.[38] Hub genes of modules associated with muscle mass and/or MPS changes were also further prioritized by those ranked in the upper quartile of their module's gene set on the basis of their individual "gene significance" (GS; |correlation coefficient|) to the given endpoint measure. Second, putative transcriptional regulators of disuse-associated modules were predicted by testing their corresponding gene lists for enriched transcription factor binding site(s) (TFBS) in the 5 kb upstream/downstream region encompassing transcription start sites. In particular, the oPOSSUM-3 webserver[54] was used to query JASPAR core vertebrae profiles with a minimum specificity of 8 bits meeting a conservation cut-off of 0.4 and similarity matrix score threshold of 85%, with the corresponding background gene list in each case constituting the genes inputted during network construction. Of note, large modules (>1000 genes) were represented by their top 75% most connected genes. Enriched TFBS were selected as those with a corresponding *Z*-score and Fisher score ≥ the mean + 1.5 SD of their respective distributions.

3 | RESULTS

3.1 | Physiologic characteristics

Thigh muscle mass tended to change over time in a leg-dependent manner (leg x time interaction $P = .076$). At baseline, thigh muscle mass did not differ between legs ($P = .424$) and remained unchanged in the control leg throughout the study ($P = .457$). However, 4 days of immobilization lead to a 1.68 ± 1.71% decrease in thigh muscle mass of the immobilized leg ($P = .036$), with daily MPS rates concomitantly 16.16 ± 9.57% lower in the immobilized leg compared to the control leg ($P = .004$). Nevertheless, as expected, inter-individual variability in physiologic responses to immobilization was observed (Figure 1), with declines in muscle mass ranging from −0.4% to 4% (Figure 1A) and concomitant MPS deficits ranging from 3% to 30% (Figure 1B).

3.2 | Gene-level expression changes following 4 days of leg immobilization

We first compared individual gene expression changes in immobilized muscle vs control muscle and identified a total of 595 genes differentially expressed between conditions (FDR < 5%), the majority of which were found to be downregulated in immobilized muscle (455 genes; Table S1). GO term enrichment analysis of differentially expressed gene sets revealed a clear ontological profile only for genes downregulated following immobilization (Figure 2A,B, Table S2). Downregulated genes were enriched for BP terms related to energy metabolism and muscle development/contraction (Figure 2A), CC terms mainly of contractile apparatus/sarcoplasmic origin (Figure 2B), and MF terms related to actin binding and ion transporter activity (Figure 2B). To provide additional functional insight of gene-level expression changes, we then determined the top-ranking up- and downregulated genes based on their log2 fold change (Figure 3)—noting several plausible candidates in the process. For example, among genes most potently upregulated by immobilization is that which encodes the well-established cytokine interleukin 18 (*IL18*). The top-ranked downregulated gene was identified to be the Leucine Rich Repeat Containing 52 gene (*LRRC52*). Several novel transcripts were also identified (Figure 3).

3.3 | Network-level expression changes following leg immobilization

To gain a systems-level understanding of the muscle transcriptional response to short-term muscle disuse, we next

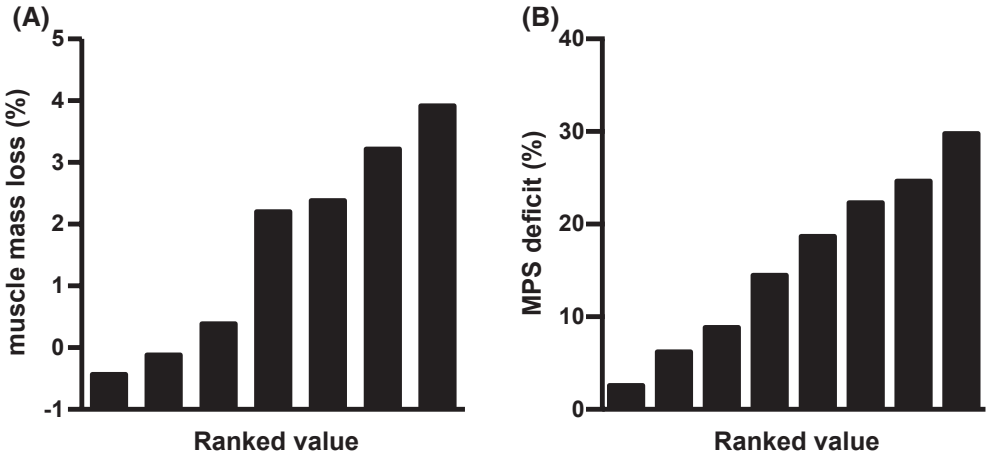

FIGURE 1 Inter-individual physiologic responsiveness to immobilization. Panel (A): Rank-ordered individual muscle mass declines (%) of the immobilized leg. Panel (B): Rank-ordered individual MPS deficits (%) with immobilization

(A)

Term ID	Description	Count	-Log10(*P*)
GO:0008015	blood circulation	31	
GO:0003013	circulatory system process	31	
GO:0034762	regulation of transmembrane transport	27	
GO:0034765	regulation of ion transmembrane transport	23	
GO:0005975	carbohydrate metabolic process	34	
GO:0016051	carbohydrate biosynthetic process	17	
GO:0044262	cellular carbohydrate metabolic process	22	
GO:0006090	pyruvate metabolic process	14	
GO:0006733	oxidoreduction coenzyme metabolic process	17	
GO:1901292	nucleoside phosphate catabolic process	16	
GO:0003012	muscle system process	36	
GO:0090257	regulation of muscle system process	18	
GO:0051146	striated muscle cell differentiation	19	
GO:0030048	actin filament-based movement	14	
GO:0006936	muscle contraction	31	
GO:0006937	regulation of muscle contraction	14	
GO:0006941	striated muscle contraction	17	
GO:0060048	cardiac muscle contraction	15	
GO:0055117	regulation of cardiac muscle contraction	10	
GO:0010882	regulation of cardiac muscle contraction by calcium ion signaling	7	
	Statistical significance scale: Biological Process		10

(B)

Term ID	Description	Count	-Log10(*P*)
GO:0043292	contractile fiber	19	
GO:0044449	contractile fiber part	19	
GO:0030016	myofibril	19	
GO:0030017	sarcomere	19	
GO:0030018	Z disc	16	
GO:0031674	I band	16	
GO:0042383	sarcolemma	13	
GO:0016528	sarcoplasm	13	
GO:0016529	sarcoplasmic reticulum	13	
GO:0033017	sarcoplasmic reticulum membrane	8	
GO:0042805	actinin binding	6	
GO:0051393	alpha-actinin binding	6	
GO:0016247	channel regulator activity	10	
GO:0022838	substrate-specific channel activity	15	
GO:0008324	cation transmembrane transporter activity	22	
GO:0022890	inorganic cation transmembrane transporter activity	21	
GO:0005267	potassium channel activity	7	
GO:0046873	metal ion transmembrane transporter activity	18	
GO:0004683	calmodulin-dependent protein kinase activity	5	
GO:0015318	inorganic molecular entity transmembrane transporter activity	31	
	Statistical significance scale: Cellular Component		10
	Statistical significance scale: Molecular Function		10

FIGURE 2 Functional enrichment of genes significantly downregulated following muscle disuse. Panel (A): Top 20 enriched Gene Ontology biological process terms for genes significantly downregulated following disuse. Panel (B): Top 10 enriched Gene Ontology cellular component (blue shading) and molecular function (green shading) terms for genes significantly downregulated following disuse. In any case, the strength of color shading depicts the magnitude of enrichment significance, given by the negative log10 of that term's enrichment FDR *P*-value (with darker shading analogous with a stronger FDR *P*-value). Terms are ordered within each category broadly by functional classes

implemented WGCNA.[48] In doing so, we identified a total of 49 distinct groups of co-regulated genes (ie, network "modules") in our dataset (Table S3), nine of which were found to have an expression profile differentially regulated by immobilization vs control (FDR < 5%; Figure 4, Table S4). Of these, seven could be subsequently labeled for function via enrichment analysis of GO terms (Figure 4, Table S5). In keeping with the overarching themes identified by gene-level differential analysis, network analysis also revealed gene signatures related to mitochondrial function (M49) and myogenesis (M35) as being downregulated in immobilized muscle. Nevertheless, network analysis also uncovered several molecular features of immobilization that were not established using standard gene-level differential analysis alone. In particular, immobilization was additionally found to upregulate muscle gene networks related to ribosome biogenesis (M2), proteasomal ubiquitin-(in)dependent protein catabolism (M28) and ribonucleoprotein complex organization/mRNA processing (M42).

3.4 | Molecular networks associated with the short-term disuse phenotype

WGCNA also facilitates discovery of the molecular signatures that underpin phenotypic change in a given state.[39]

Ensembl ID	Gene Symbol	Description	Log2 FC	-Log10(*P*)
ENSG00000138435	*CHRNA1*	Cholinergic Receptor Nicotinic Alpha 1 Subunit	1.52	
ENSG00000205056	*LINC02397*	Long Intergenic Non-Protein Coding RNA 2397	1.34	
ENSG00000168621	*GDNF*	Glial Cell Derived Neurotrophic Factor	1.33	
ENSG00000188522	*FAM83G*	Family With Sequence Similarity 83 Member G	1.21	
ENSG00000285873		Novel transcript	1.19	
ENSG00000150782	*IL18*	Interleukin 18	1.19	
ENSG00000258584	*FAM181A-AS1*	FAM181A Antisense RNA 1	1.19	
ENSG00000145107	*TM4SF19*	Transmembrane 4 L Six Family Member 19	1.16	
ENSG00000120658	*ENOX1*	Ecto-NOX Disulfide-Thiol Exchanger 1	1.15	
ENSG00000257829		Novel Transcript, Antisense To KRT86	1.12	
ENSG00000162763	*LRRC52*	Leucine Rich Repeat Containing 52	-2.71	
ENSG00000185669		Snail Family Transcriptional Repressor 3	-2.48	
ENSG00000199017	*MIR1-1*	MicroRNA 1-1	-2.24	
ENSG00000118298	*CA14*	Carbonic Anhydrase 14	-2.20	
ENSG00000286272		Novel transcript	-2.01	
ENSG00000271952	*LINC01954*	Long Intergenic Non-Protein Coding RNA 1954	-1.99	
ENSG00000158486	*DNAH3*	Dynein Axonemal Heavy Chain 3	-1.98	
ENSG00000261303		Golgin Subfamily A Pseudogene	-1.93	
ENSG00000224328	*MDC1-AS1*	MDC1 Antisense RNA 1	-1.87	
ENSG00000211750	*TRBV24-1*	T Cell Receptor Beta Variable 24-1	-1.81	
		Statistical significance scale: upregulated		10
		Statistical significance scale: downregulated		10

FIGURE 3 Top ranking differentially expressed genes following muscle disuse. Top 10 significantly upregulated (red shading) and downregulated (blue shading) genes, as based on log2 fold change (log2 FC). Strength of shading depicts the magnitude of significant differential expression for a given gene, given by the negative log10 of its FDR *P*-value (with darker shading corresponding to a stronger FDR *P*-value)

Capitalizing on the observed heterogeneity in muscle physiologic responses, we used WGCNA to identify network modules with expression change correlating with muscle mass/MPS declines. We identified a total of four network modules that were regulated in proportion to the extent of muscle lost after immobilization (M5, M15, M20, and M31) and a further three that were regulated in proportion to the magnitude of MPS suppression (M8, M10, and M33) (Figure 4, Table S4). Of those modules regulated in proportion to muscle mass declines, one had expression positively scaling with the extent of muscle mass lost (M15) and was enriched for genes involved in mitochondria function. The remaining muscle mass-related modules all had expression negatively scaling with the magnitude of muscle mass lost and were enriched for genes involved in protein folding (M5), histone acetyltransferase activity (M20), and extracellular matrix (ECM) organization (M31). All three MPS-related network modules had expression positively scaling with the extent of MPS suppression following disuse. Of these, only one could be labeled for function via enrichment analysis of GO terms (M10—ubiquitin-protein transferase activity).

3.5 | Network-driven identification of key disuse-associated candidates

We established key molecular drivers of the short-term muscle disuse phenotype by searching for highly connected "hub" genes within disuse-associated modules.[53] In doing so, we identified 242 module hubs from 7158 genes across the 15 disuse-associated network modules (Table S6). Notably, the top-ranked hub gene of each module regulated in proportion to the extent of muscle mass (Figure 5) or MPS declines (Figure 6) was also found to be strongly associated with consequent muscle mass/MPS decrements following immobilization (Figures 5 and 6). These particular seven genes (*AGO2*, *ADAMTS2*, *DEPTOR*, *FOXO3B*, *LRRC30*, *MTATP6P1*, and *TP53BP1*), along with the other module hubs that tightly connect to muscle mass/MPS declines (Figures 5 and 6), thus

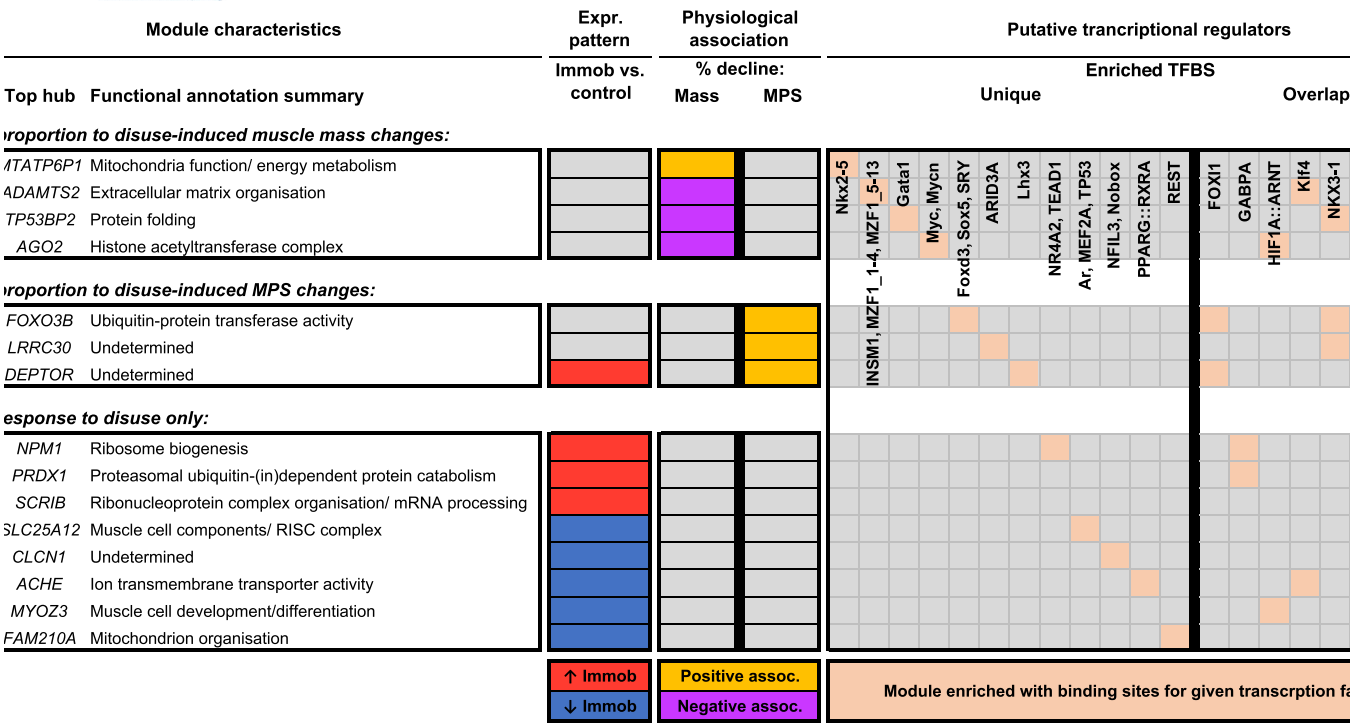

FIGURE 4 Muscle disuse-associated network modules and molecular candidates. Modules shown are those differentially regulated by disuse and/or regulated in proportion to the extent of muscle mass lost/MPS suppression with disuse. Red and blue shading denote significant upregulation and downregulation following immobilization (immob; vs control), respectively. Orange and purple shading depict a significant positive or negative correlation between a given module's expression pattern change (Δ; immob minus control) and percent loss of the given physiological variable, respectively. Also provided is each module's top ranked hub gene and transcription factors with enriched binding site(s) (TFBS)

represent strong *physiologically relevant* mechanistic candidates in the context of short-term disuse atrophy.

3.6 | Putative transcriptional regulators of co-expression

Finally, we established putative regulatory factors driving co-expression of disuse-associated modules, by searching module genes for conserved TFBS.[54] A core set of 31 putative transcriptional regulators was subsequently identified, with each pertinent module displaying enrichment for at least one TFBS (Figure 4). Interestingly, just over two-thirds (21 of the 31) of the identified transcription factors were predicted to regulate only a single of the disuse-associated network modules, perhaps implicating the upstream mechanisms that regulate critical molecular responses during short-term muscle disuse are largely unique. Moreover, within six of the seven muscle mass/MPS-related modules, most of the hub genes strongly associated with muscle mass/MPS declines were predicted to contain a binding site for at least one of the predicted transcription factors for that module (Figures 5 and 6). In module M15 (mitochondria function), just one of the hub genes (*DLD*) was predicted to contain a binding site for this module's only predicted transcription factor (NKX2-5). Overall, these specific transcription factors may therefore play a central role in the mediating molecular mechanisms of short-term disuse atrophy.

4 | DISCUSSION

Periods of short-term muscle disuse occur regularly throughout life (eg, with minor injury or illness) and often result in muscle atrophy,[6,7] with the amalgamation of such short periods of muscle disuse consequently regarded as an important driver of sarcopenia.[6] Nevertheless, irrespective of age, the mechanisms that underlie short-term disuse atrophy remain poorly defined, hindering the development of optimal preventative strategies that might in turn help to mitigate sarcopenic progression. Here, for the first time, this study combined robust muscle morphological (muscle mass) and metabolic (MPS) assessment with data-driven network analysis to elucidate new mechanistic candidates of short-term disuse atrophy in humans, namely by establishing molecular networks and key regulatory molecules *quantitatively linked* to muscle mass and/or MPS changes following 4 days of immobilization.

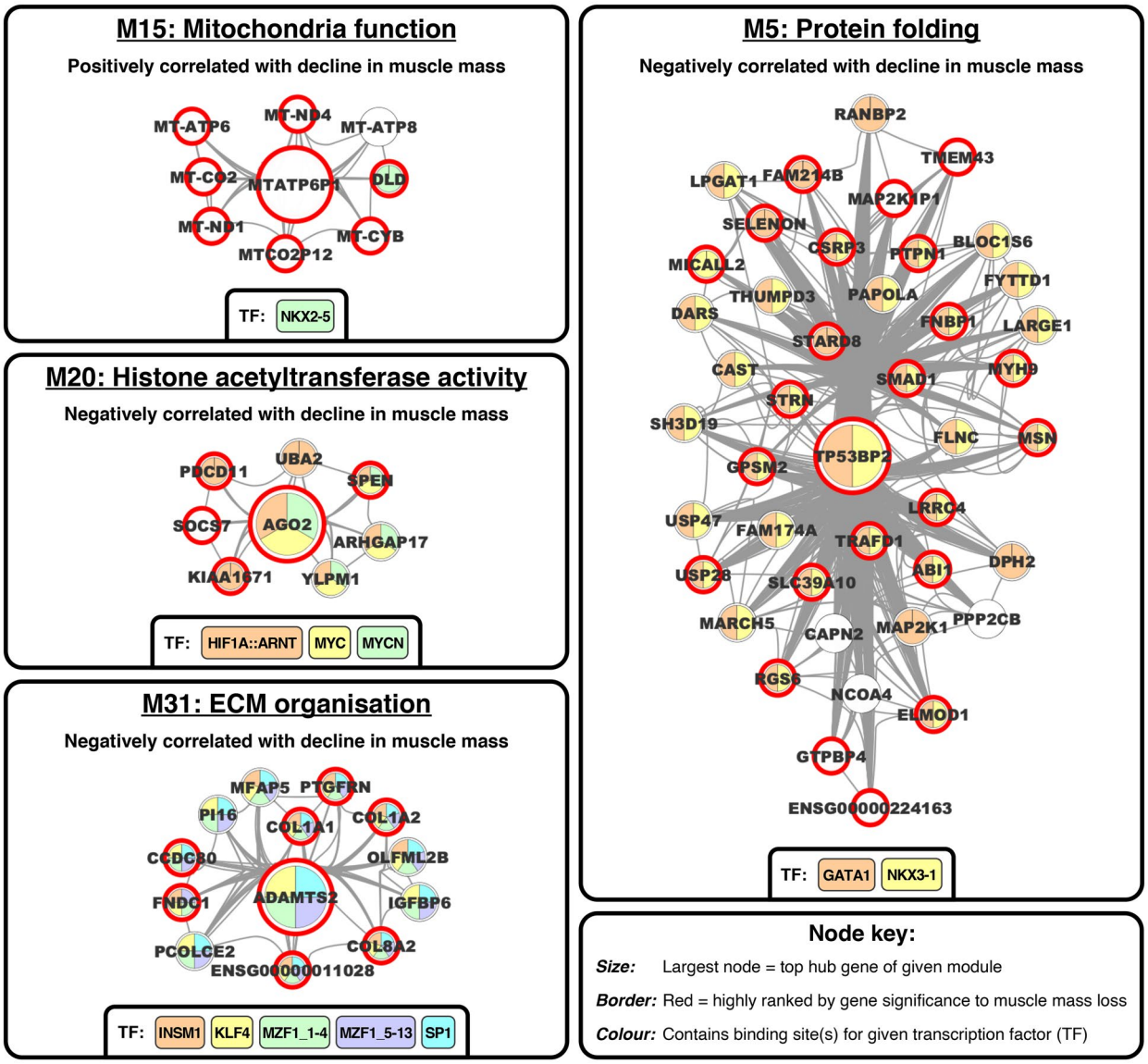

FIGURE 5 Hub gene networks for modules regulated in proportion to the extent of muscle mass lost with disuse. Each network visualization comprises all corresponding hub genes of the given module, with the top ranked hub gene given by a larger node. Red borders illustrate hub genes within each module that are also highly linked to the extent of mass loss (ie, within the upper quartile of corresponding module's genes ranked by their gene significance to declines in mass), with node fill colors illustrating whether the corresponding hub gene is among the module genes that are enriched with binding site(s) for the given transcription factor (TF). Visualizations were generated using Cytoscape (v3.7.1)[92]

Muscle loss ensues at a rapid rate following the onset of disuse, occurring in a matter of days,[7,55] although there does exist notable inter-individual variability,[7,31] implying that regulation of short-term disuse atrophy is heterogeneous. Consistent with this, we identified a number of molecular networks that were not globally regulated by disuse per se, but rather, were "activated" directly in proportion to the extent of disuse muscle atrophy experienced. Networks that showed the greatest expression reduction in proportion to losses of muscle mass were enriched for genes involved in ECM organization (M31), protein folding (M5), and histone acetyltransferase activity (M20). In recent network analyses of a multi-study tissue biobank, Stokes et al similarly show that gene networks centered upon ECM remodeling form to become a top feature in muscle under different loading states,[34] with decreased ECM gene expression being further noted in both rodent and human models of short-term immobilization.[29,56] ECM remodeling and protein folding, in particular, are both highly mechanosensitive events, and consequently, play a central role in regulating muscle mass by maintaining structural integrity as well as via downstream mechanotransduction of other signaling cascades responsible for muscle growth/maintenance.[57-60] Collectively, such

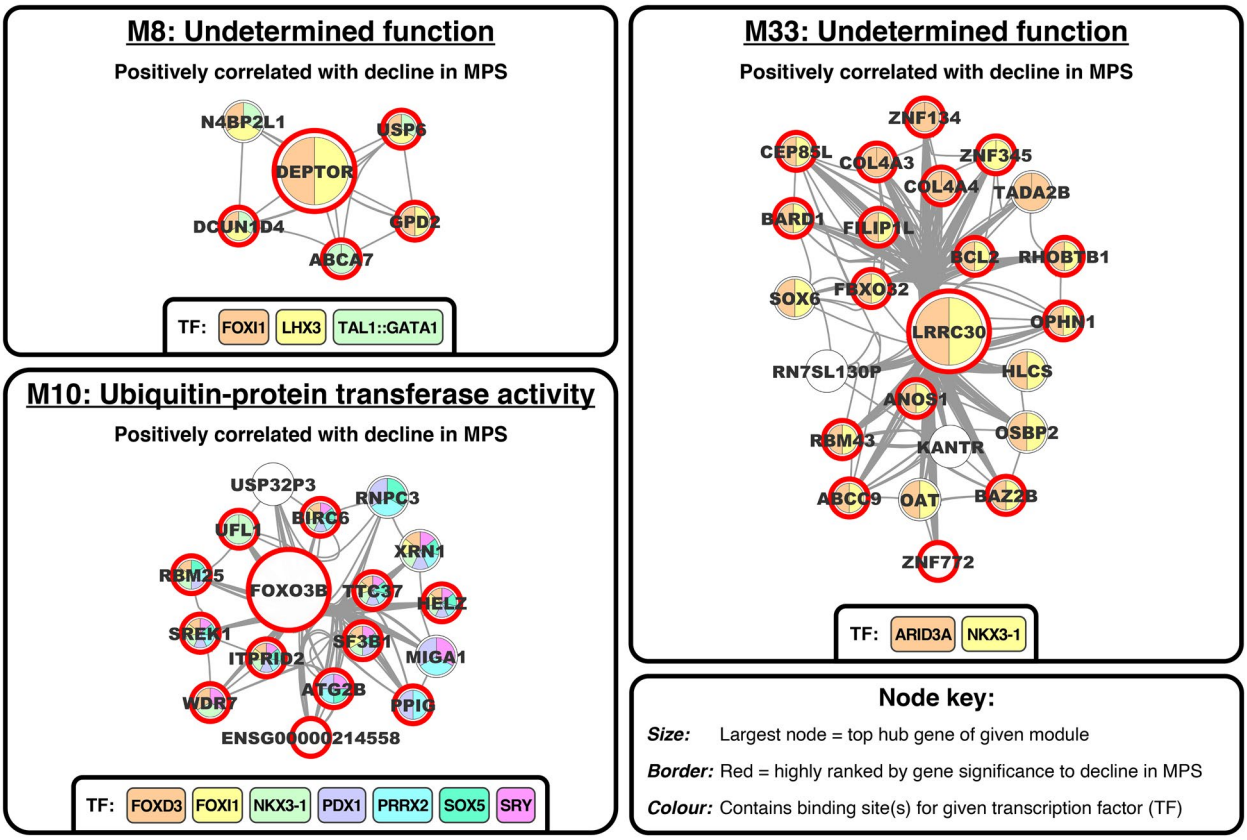

FIGURE 6 Hub gene networks for modules regulated in proportion to the extent of MPS suppression with disuse. Each network visualization comprises all corresponding hub genes of the given module, with the top ranked hub gene given by a larger node. Red borders illustrate hub genes within each module that are also highly linked to the extent of MPS decline (ie, within the upper quartile of corresponding module's genes ranked by their gene significance to declines in MPS), with node fill colors illustrating whether the corresponding hub gene is among the module genes that are enriched with binding site(s) for the given transcription factor (TF). Visualizations were generated using Cytoscape (v3.7.1)[92]

findings indicate that the downregulation of processes involved in muscle structural dynamics is part of potent intrinsic mechanisms contributing to short-term disuse atrophy, presumably as a direct result of the musculature rapidly adapting to alterations in muscle loading.

Unloading also plays a fundamental role in regulating MPS,[61-63] the decrement in which is proposed to be the dominant mechanism underpinning short-term disuse atrophy.[23] Here, we obtained D_2O-derived measurements of MPS to assess integrated MPS changes across the *entire* period of disuse, in contrast to traditional "acute" (ie, stable isotopically labeled amino acid infusion) tracer methods.[35,64] The D_2O method remains novel in human disuse research.[26,65] Exploiting this approach in tandem with untargeted transcriptomic profiling thus provided a powerful basis through which to *directly connect* key molecular and MPS changes and, in turn, identify new mechanistic candidates of disuse-induced MPS suppression. In doing so, we identified a molecular network that was both activated by disuse *and* positively correlated with declines in MPS (M8)—that is, those with greater upregulation of this network also experienced a greater suppression of MPS. While this network demonstrated no particular ontological annotation, the top-ranked "hub" gene was *DEPTOR*, which is a potent inhibitor of mTOR:[66] a regulatory complex through which MPS is positively controlled in response to mechanical (un) loading.[67] Work in rodents has shown DEPTOR activity to be tightly linked to MPS,[68] with DEPTOR knockdown ameliorating disuse atrophy in vivo via enhanced MPS.[69] However, to our knowledge the current study is the first to provide evidence for DEPTOR as a key mechanistic target of disuse driven MPS suppression directly in humans. While presumably mTOR related, the precise action by which DEPTOR might inhibit MPS during short-term disuse warrants elucidation. Indeed, DEPTOR is a common inhibitory component of both mTOR complexes 1 and 2 (mTORC1/2),[70-72] and could thus theoretically inhibit MPS during disuse directly upstream of Akt (via mTORC2 inhibition), at the intersection of Akt and mTORC1 (via PRAS40 inhibition), and/or directly at the level of mTORC1 (ie, independent of

Akt altogether).[69-72] Nevertheless, augmentation of both 4E-BP1 and S6K1 signaling upon DEPTOR knockdown[69] suggests that DEPTOR may suppress MPS during disuse by impairing both translation initiation and elongation. Given that this network was not associated with muscle mass changes, it remains to be established how any such DEPTOR-induced MPS suppression might relate to corresponding atrophy. Nonetheless, our direct linking of transcriptomics to MPS suggests DEPTOR-dependent, mTOR-related suppression of MPS could be an important mechanism of atrophy during disuse in humans.

Two additional molecular networks were found to quantitatively connect to alterations in MPS, with both tending to display greater expression increases in subjects with a more pronounced decline in MPS (M10—ubiquitin-protein transferase activity, M33—undetermined function). Interestingly, more than half of the top-ranked hub genes contained within M10 putatively serve to function in proteolytic-related pathways (*FOXO3B*, *ATG2B*, *WDR7*, *TTC37*, *RBM25*, *BIRC6*, and *UFL1*),[73] while *FBXO32* (ie, MAFbx/Atrogin-1) was among the top-ranked hub genes of M33. The untargeted identification of *FBXO32* is particularly striking, given that it is widely considered a universal atrophy-related gene ("atrogene") involved in initiating proteolysis across a wide range of catabolic conditions[74] and is unsurprisingly found upregulated often in human models of simple disuse.[26,27,55,75-78] Nevertheless, our data extend beyond previous studies by suggesting a central regulatory role for FBXO32 in suppressing MPS during short-term human disuse atrophy. More generally, our above-mentioned data seem to imply an associative link between increased proteolytic marker expression—and thus ostensibly MPB processes—and declines in MPS during short-term disuse. Whether or not MPB plays a direct role in human muscle disuse atrophy remains up for debate. Secondary evidence for increased MPB during human disuse can indeed be derived from other "static" markers of myofibrillar breakdown (eg, increased interstitial 3-methylhistidine and proteasomal/lysosomal molecule expression).[26,77,79] On the other hand, both model-derived and direct quantifications, although scant, have found no appreciable change in "bulk" MPB,[80,81] with mathematical estimates further showing that attenuated MPS alone is sufficient to explain muscle loss during disuse.[23,25] Thus, if observed increases in markers of MPB play a mechanistic role in human disuse atrophy, it seems likely to be beyond functionally regulating bulk myofibrillar proteolysis, which itself does not appear to be a necessity of human disuse atrophy. An alternative contention which may then both explain and be supported by our current data is that increases in static markers of MPB are actually acting to degrade specific components of the protein-synthetic machinery (and thus regulating the capacity for MPS), rather than regulating bulk MPB per se.[14] This indeed seems plausible especially in the case of FBXO32, which holds a strong potential to suppress MPS during disuse via degradation of EIF-3F: an essential protein in instigating translation initiation.[14] Although, such inferences should remain taken with caution given the lack of available data that currently exists on dynamic MPB changes during human disuse as opposed to changes in MPS.[14,15]

It is also important to acknowledge those molecular networks that did not link to muscle mass/MPS changes but were nevertheless found to be regulated in direct response to the disuse intervention. Such networks could theoretically contribute to short-term disuse atrophy via mechanisms beyond those we have considered and/or be molecular events that precede atrophy occurring beyond 4 days of disuse. Of note are the functional expression patterns that remained consistent across both our differential module-level and gene-level analyses; namely the concordant downregulation of genes functionally related to mitochondrial function, muscle cell differentiation and ion transmembrane transporter activity. Tight coordination of the mitochondrial transcriptome corroborates with recent large-scale network analysis of differential muscle loading responses to resistance training/immobilization, in spite of a longer duration of disuse (14 days) having been employed.[34] In fact, downregulation of mitochondria-related genes appears a general feature of muscle disuse (ie, independent of duration or model),[28-30,82,83] and on the whole is likely indicative of a disuse-induced impairment in mitochondrial function. The downregulation of genes involved in ion transmembrane transporter activity was also notable, given that it remains a relatively novel finding in the context of human muscle disuse. Interestingly, the top-ranking hub gene of this specific molecular network was identified as *ACHE*, the primary function of which is to hydrolyze acetylcholine at neuromuscular junctions. ACHE deficiency is associated with impaired neuromuscular junction function in the form of reduced neuromuscular transmission.[84] The possible physiological relevance of this specific network is thus perhaps more likely to lie within the realms of disuse-induced muscle dysfunction (eg, impaired muscle contractibility).

Worthwhile appraising are the relative merits of our study design. By subjecting healthy younger individuals to disuse via ULLI, we were able to isolate the effects of disuse on muscle tissue per se independently of any comorbid factors. By integrating muscle mass and MPS measurements with network-driven analysis, we were subsequently able to generate new insight into potential pathways and key molecules associated with the short-term human muscle disuse phenotype; crucially, direct links between MPS deficits and both *DEPTOR* and molecular

MPB biomarker upregulation. Nevertheless, we acknowledge that our design of comparing end-intervention biopsies between legs to assess immobilization effects could, in theory, be complicated by having a weight bearing "control" limb that is supporting more of a person's bodyweight. In which instance, we would be comparing biopsies from a limb bearing more weight to one bearing no weight and thus the non-immobilized leg biopsy would not be a true control nor our model consequently a true representation of immobilization per se. While we cannot discount such a possibility, if this were indeed the case then it might be reasonable to postulate improved conditioning in the non-immobilized leg. Regarding our physiologic variables, however, in line with others,[7,85,86] muscle mass was unchanged in the non-immobilized leg herein, with further evidence demonstrating that D_2O-derived integrative MPS rates remain stable over 7 days in a non-immobilized leg while declining in the immobilized leg.[26] Equally, it may even be that the non-immobilized leg is bearing less weight across the immobilization phase of the study as people on crutches simply do less and are more sedentary as the work of ambulation on crutches is taxing compared to normal ambulation. Some support for this comes from our previous observation that both legs during a ULLI model showed evidence of reduced vascular response to shear stress, demonstrating at least some level of deconditioning can take place in both limbs.[87] Evidence also shows that muscles, including the *m. vastus lateralis*, can do less work (ie, reduced loading) during crutching and single-leg immobilization and thus may not necessary always be loaded to a greater extent.[88] Either way, however, it is likely that initial responses of the immobilized and non-immobilized leg muscles are manifest at the mRNA level. As a result, we cannot fully exclude the possibility of some transcriptomic perturbation having occurred in the non-immobilized leg (convergent, divergent, or even entirely distinct from the immobilized leg) if it was in fact either over- or under-loaded throughout, and which theoretically could have still arisen in spite of muscle mass (and plausibly MPS) of this leg remaining stable. Relatedly, given the number of genes analyzed, the potential for at least some within-individual molecular variability and/or cross-leg "transfer" response also cannot be ruled out entirely. Clearly, to resolve these issues we could have taken a baseline biopsy from each leg to derive and compare temporal mRNA changes in each leg. Without these biopsies we thus acquiesce that our results might not provide an entirely clear transcriptomic interpretation of the impact of immobilization per se and further work should add pre-intervention biopsies to account for the potential confounding of using a post-intervention biopsy from the non-immobilized leg as a control.

We also recognize a further need for caution when inferring true intervention effects of this work due to the relatively small number of individuals that were included herein. Although, the number of samples used was within the WGCNA developers recommendations,[89] and the network approaches employed shown to perform strongly even when applied to smaller (~20 samples)/paired design datasets.[90,91] Thus, while further work incorporating larger cohort sizes and deeper quantitative/mechanistic investigation is ultimately warranted as a next step, a major novel outcome of our current work is the network-driven identification of an *experimentally tractable* set of *physiologically relevant* mechanistic targets: key candidates that *quantitatively connect* to the primary physiological/metabolic consequences of muscle disuse—that is, muscle atrophy and blunted MPS. Our findings therefore offer a strong benchmark to expedite mechanistic understanding of short-term human disuse atrophy and, in turn, may help to accelerate the development of effective countermeasure approaches.

ACKNOWLEDGMENTS

The authors thank all of the volunteers for giving up their time to partake in the human clinical experiment. Craig R. G. Willis is supported by the Biotechnology and Biological Sciences Research Council-funded South West Biosciences Doctoral Training Partnership (BB/J014400/1; BB/M009122/1). Tanner Stokes is supported by the Alexander Graham Bell Canadian Graduate Scholarship from the Natural Sciences and Engineering Research Council. This work was partially supported by funding from the Biotechnology and Biological Sciences Research Council (BB/N015894/1). This research was also supported by the MRC-Versus Arthritis Centre for Musculoskeletal Ageing Research (MR/P021220/1; MR/R502364/1) and National Institute for Health Research Nottingham Biomedical Research Centre. The views expressed are those of the author(s) and not necessarily those of the NHS, the NIHR or the Department of Health and Social Care.

DISCLOSURES

SMP reports that he is an inventor on a patent (WO/2018/157258) held by Exerkine Corporation and holds equity in Exerkine (all proceeds donated to charity). SMP is a member, and receives an honorarium, of the scientific advisory board of Enhanced Recovery (https://ersportsdrink.com/; all proceeds donated to charity). SMP has received, in the last 5 years, honoraria and travel expenses from the US National Dairy Council, the National Cattlemen's Beef Association, and the US Dairy Export Council. The other authors declare that they have no conflicts of interest.

AUTHOR CONTRIBUTIONS

All authors contributed to the conception or design of the research. TS, CM, SHMG, and SMP conducted the human clinical experiment. DJW, MSB, JJB, BEP, and KS contributed to sample analysis. CRGW and IJG performed the bioinformatic analysis. CRGW, IJG, and PJA interpreted the data and drafted the initial manuscript. All authors reviewed, edited, and approved the final manuscript.

REFERENCES

1. Dirks ML, Backx EMP, Wall BT, Verdijk LB, van Loon LJC. May bed rest cause greater muscle loss than limb immobilization? *Acta Physiol*. 2016;218(1):10-12. https://doi.org/10.1111/apha.12699
2. Fitts RH, Trappe SW, Costill DL, et al. Prolonged space flight-induced alterations in the structure and function of human skeletal muscle fibres. *J Physiol*. 2010;588(Pt 18):3567-3592. https://doi.org/10.1113/jphysiol.2010.188508
3. Homma T, Hamaoka T, Murase N, et al. Low-volume muscle endurance training prevents decrease in muscle oxidative and endurance function during 21-day forearm immobilization. *Acta Physiol*. 2009;197(4):313-320. https://doi.org/10.1111/j.1748-1716.2009.02003.x
4. Dirks ML, Wall BT, van de Valk B, et al. One week of bed rest leads to substantial muscle atrophy and induces whole-body insulin resistance in the absence of skeletal muscle lipid accumulation. *Diabetes*. 2016;65(10):2862-2875. https://doi.org/10.2337/db15-1661
5. Wall BT, Dirks ML, Snijders T, et al. Short-term muscle disuse lowers myofibrillar protein synthesis rates and induces anabolic resistance to protein ingestion. *Am J Physiol Endocrinol Metab*. 2016;310(2):E137-E147. https://doi.org/10.1152/ajpendo.00227.2015
6. Wall BT, Dirks ML, Van Loon LJC. Skeletal muscle atrophy during short-term disuse: Implications for age-related sarcopenia. *Ageing Res Rev*. 2013;12(4):898-906. https://doi.org/10.1016/j.arr.2013.07.003
7. Kilroe SP, Fulford J, Jackman SR, Van loon LJC, Wall BT. Temporal muscle-specific disuse atrophy during one week of leg immobilization. *Med Sci Sports Exerc*. 2020;52(4):944-954. https://doi.org/10.1249/MSS.0000000000002200
8. Fisher SR, Kuo Y, Graham JE, Ottenbacher KJ, Ostir GV. Early ambulation and length of stay in older adults hospitalized for acute illness. *Arch Intern Med*. 2010;170(21):1942-1943. https://doi.org/10.1001/archinternmed.2010.422
9. World Health Organization. *Average Length of Stay, All Hospitals*. 2019. https://gateway.euro.who.int/en/indicators/hfa_540-6100-average-length-of-stay-all-hospitals/. Accessed June 25, 2020.
10. Tully MA, Bleakley CM, O'Connor SR, McDonough SM. Functional management of ankle sprains: what volume and intensity of walking is undertaken in the first week postinjury. *Br J Sports Med*. 2012;46(12):877-882. https://doi.org/10.1136/bjsports-2011-090692
11. NHS Digital. *Hospital Admitted Patient Care and Adult Critical Care Activity*. 2019. https://files.digital.nhs.uk/F2/E70669/hosp-epis-stat-admi-summ-rep-2018-19-rep.pdf. Accessed August 14, 2020.
12. Institute for Government. *Hospitals*. 2019. https://www.instituteforgovernment.org.uk/publication/performance-tracker-2019/hospitals. Accessed June 25, 2020.
13. World Health Organization. *Ageing and Health*. 2018. https://www.who.int/en/news-room/fact-sheets/detail/ageing-and-health. Accessed June 25, 2020.
14. Atherton PJ, Greenhaff PL, Phillips SM, et al. Control of skeletal muscle atrophy in response to disuse: clinical/preclinical contentions and fallacies of evidence. *Am J Physiol Endocrinol Metab*. 2016;311(3):E594-E604. https://doi.org/10.1152/ajpendo.00257.2016
15. Rudrappa SS, Wilkinson DJ, Greenhaff PL, et al. Human skeletal muscle disuse atrophy: effects on muscle protein synthesis, breakdown, and insulin resistance—a qualitative review . *Front Physiol*. 2016;7:361. https://doi.org/10.3389/fphys.2016.00361
16. Lee CG, Boyko EJ, Strotmeyer ES, et al. Association between insulin resistance and lean mass loss and fat mass gain in older men without diabetes mellitus. *J Am Geriatr Soc*. 2011;59(7):1217-1224. https://doi.org/10.1111/j.1532-5415.2011.03472.x
17. Londhe P, Guttridge DC. Inflammation induced loss of skeletal muscle. *B one*. 2015;80:131-142. https://doi.org/10.1016/j.bone.2015.03.015
18. Evans WJ. Skeletal muscle loss: cachexia, sarcopenia, and inactivity. *Am J Clin Nutr*. 2010;91(4):1123S-1127S. https://doi.org/10.3945/ajcn.2010.28608A
19. Odegaard JI, Chawla A. Pleiotropic actions of insulin resistance and inflammation in metabolic homeostasis. *Science*. 2013;339(6116):172-177. https://doi.org/10.1126/science.1230721
20. Dirks ML, Wall BT, van Loon LJC. Interventional strategies to combat muscle disuse atrophy in humans: focus on neuromuscular electrical stimulation and dietary protein. *J Appl Physiol*. 2018;125(3):850-861. https://doi.org/10.1152/japplphysiol.00985.2016
21. Dirks ML, Wall BT, Otten B, et al. High-fat overfeeding does not exacerbate rapid changes in forearm glucose and fatty acid balance during immobilization. *J Clin Endocrinol Metab*. 2020;105(1):1-14. https://doi.org/10.1210/clinem/dgz049
22. Brook MS, Wilkinson DJ, Phillips BE, et al. Skeletal muscle homeostasis and plasticity in youth and ageing: impact of nutrition and exercise. *Acta Physiol*. 2016;216(1):15-41. https://doi.org/10.1111/apha.12532
23. Phillips SM, McGlory C. CrossTalk proposal: the dominant mechanism causing disuse muscle atrophy is decreased protein synthesis. *J Physiol*. 2014;592(24):5341-5343. https://doi.org/10.1113/jphysiol.2014.273615
24. Holloway TM, McGlory C, McKellar S, et al. A novel amino acid composition ameliorates short-term muscle disuse atrophy in healthy young men. *Front Nutr*. 2019;6:105. https://doi.org/10.3389/fnut.2019.00105
25. De Boer MD, Selby A, Atherton P, et al. The temporal responses of protein synthesis, gene expression and cell signalling in human quadriceps muscle and patellar tendon to disuse. *J Physiol*. 2007;585(Pt 1):241-251. https://doi.org/10.1113/jphysiol.2007.142828
26. Kilroe SP, Fulford J, Holwerda AM, et al. Short-term muscle disuse induces a rapid and sustained decline in daily myofibrillar protein synthesis rates. *Am J Physiol Endocrinol Metab*. 2020;318(2):E117-E130. https://doi.org/10.1152/ajpendo.00360.2019

27. Gustafsson T, Osterlund T, Flanagan JN, et al. Effects of 3 days unloading on molecular regulators of muscle size in humans. *J Appl Physiol*. 2010;109(3):721-727. https://doi.org/10.1152/japplphysiol.00110.2009
28. Reich KA, Chen Y-W, Thompson PD, Hoffman EP, Clarkson PM. Forty-eight hours of unloading and 24 h of reloading lead to changes in global gene expression patterns related to ubiquitination and oxidative stress in humans. *J Appl Physiol*. 2010;109(5):1404-1415. https://doi.org/10.1152/japplphysiol.00444.2010
29. Urso ML, Scrimgeour AG, Chen Y-W, Thompson PD, Clarkson PM. Analysis of human skeletal muscle after 48 h immobilization reveals alterations in mRNA and protein for extracellular matrix components. *J Appl Physiol*. 2006;101(4):1136-1148. https://doi.org/10.1152/japplphysiol.00180.2006
30. Abadi A, Glover EI, Isfort RJ, et al. Limb immobilization induces a coordinate down-regulation of mitochondrial and other metabolic pathways in men and women. *PLoS ONE*. 2009;4(8):e6518. https://doi.org/10.1371/journal.pone.0006518
31. Yasuda N, Glover EI, Phillips SM, Isfort RJ, Tarnopolsky MA. Sex-based differences in skeletal muscle function and morphology with short-term limb immobilization. *J Appl Physiol*. 2005;99(3):1085-1092. https://doi.org/10.1152/japplphysiol.00247.2005
32. Phillips BE, Williams JP, Gustafsson T, et al. Molecular networks of human muscle adaptation to exercise and age. *PLoS Genet*. 2013;9(3):e1003389. https://doi.org/10.1371/journal.pgen.1003389
33. Thalacker-Mercer A, Stec M, Cui X, et al. Cluster analysis reveals differential transcript profiles associated with resistance training-induced human skeletal muscle hypertrophy. *Physiol Genomics*. 2013;45(12):499-507. https://doi.org/10.1152/physiolgenomics.00167.2012
34. Stokes T, Timmons JA, Crossland H, et al. Molecular transducers of human skeletal muscle remodeling under different loading states. *Cell Rep*. 2020;32(5):107980. https://doi.org/10.1016/j.celrep.2020.107980
35. Wilkinson DJ, Franchi MV, Brook MS, et al. A validation of the application of D(2)O stable isotope tracer techniques for monitoring day-to-day changes in muscle protein subfraction synthesis in humans. *Am J Physiol Endocrinol Metab*. 2014;306(5):E571-E579. https://doi.org/10.1152/ajpendo.00650.2013
36. Franchi MV, Wilkinson DJ, Quinlan JI, et al. Early structural remodeling and deuterium oxide-derived protein metabolic responses to eccentric and concentric loading in human skeletal muscle. *Physiol Rep*. 2015;3(11):e12593. https://doi.org/10.14814/phy2.12593
37. Brook MS, Wilkinson DJ, Mitchell WK, et al. Skeletal muscle hypertrophy adaptations predominate in the early stages of resistance exercise training, matching deuterium oxide-derived measures of muscle protein synthesis and mechanistic target of rapamycin complex 1 signaling. *FASEB J*. 2015;29(11):4485-4496. https://doi.org/10.1096/fj.15-273755
38. Willis CRG, Ames RM, Deane CS, et al. Network analysis of human muscle adaptation to aging and contraction. *Aging*. 2020;12(1):740-755. https://doi.org/10.18632/aging.102653
39. van Dam S, Võsa U, van der Graaf A, Franke L, de Magalhães JP. Gene co-expression analysis for functional classification and gene-disease predictions. *Brief Bioinform*. 2018;19(4):575-592. https://doi.org/10.1093/bib/bbw139
40. Bergström J. Percutaneous needle biopsy of skeletal muscle in physiological and clinical research. *Scand J Clin Lab Invest*. 1975;35(7):609-616. https://doi.org/10.1080/00365517509095787
41. Brook MS, Wilkinson DJ, Mitchell WK, et al. Synchronous deficits in cumulative muscle protein synthesis and ribosomal biogenesis underlie age-related anabolic resistance to exercise in humans. *J Physiol*. 2016;594(24):7399-7417. https://doi.org/10.1113/JP272857
42. Liao Y, Smyth GK, Shi W. The R package Rsubread is easier, faster, cheaper and better for alignment and quantification of RNA sequencing reads. *Nucleic Acids Res*. 2019;47(8):e47. https://doi.org/10.1093/nar/gkz114
43. Robinson MD, McCarthy DJ, Smyth GK. edgeR: a Bioconductor package for differential expression analysis of digital gene expression data. *Bioinformatics*. 2010;26(1):139-140. https://doi.org/10.1093/bioinformatics/btp616
44. Lun ATL, Chen Y, Smyth GK. It's DE-licious: a recipe for differential expression analyses of RNA-seq experiments using quasi-likelihood methods in edgeR. *Methods Mol Biol*. 2016;1418:391-416. https://doi.org/10.1007/978-1-4939-3578-9_19
45. Langfelder P, Horvath S. WGCNA: an R package for weighted correlation network analysis. *BMC Bioinformatics*. 2008;9:559. https://doi.org/10.1186/1471-2105-9-559
46. Anders S, Huber W. Differential expression analysis for sequence count data. *Genome Biol*. 2010;11(10):r106. https://doi.org/10.1186/gb-2010-11-10-r106
47. Mason MJ, Fan G, Plath K, Zhou Q, Horvath S. Signed weighted gene co-expression network analysis of transcriptional regulation in murine embryonic stem cells. *BMC Genom*. 2009;10:327. https://doi.org/10.1186/1471-2164-10-327
48. Zhang B, Horvath S. A general framework for weighted gene co-expression network analysis. *Stat Appl Genet Mol Biol*. 2005;4(1):Article17. https://doi.org/10.2202/1544-6115.1128
49. Langfelder P, Zhang B, Horvath S. Defining clusters from a hierarchical cluster tree: the Dynamic Tree Cut package for R. *Bioinformatics*. 2008;24(5):719-720. https://doi.org/10.1093/bioinformatics/btm563
50. Oldham MC. From differential expression to coexpression. In: Coppola G, ed. *The OMICs: Applications in Neuroscience*. Oxford University Press; 2014:85-113.
51. Ritchie ME, Phipson B, Wu DI, et al. limma powers differential expression analyses for RNA-sequencing and microarray studies. *Nucleic Acids Res*. 2015;43(7):e47. https://doi.org/10.1093/nar/gkv007
52. Yu G, Wang L-G, Han Y, He Q-Y. clusterProfiler: an R package for comparing biological themes among gene clusters. *OMICS*. 2012;16(5):284-287. https://doi.org/10.1089/omi.2011.0118
53. Horvath S, Dong J. Geometric interpretation of gene coexpression network analysis. *PLoS Comput Biol*. 2008;4(8):e1000117. https://doi.org/10.1371/journal.pcbi.1000117
54. Kwon AT, Arenillas DJ, Worsley Hunt R, Wasserman WW. oPOSSUM-3: advanced analysis of regulatory motif over-representation across genes or ChIP-Seq datasets. *G3*. 2012;2(9):987-1002. https://doi.org/10.1534/g3.112.003202
55. Wall BT, Dirks ML, Snijders T, et al. Substantial skeletal muscle loss occurs during only 5 days of disuse. *Acta Physiol*. 2014;210(3):600-611. https://doi.org/10.1111/apha.12190
56. Stevenson EJ, Giresi PG, Koncarevic A, Kandarian SC. Global analysis of gene expression patterns during disuse atrophy in

rat skeletal muscle. *J Physiol*. 2003;551(Pt 1):33-48. https://doi.org/10.1113/jphysiol.2003.044701

57. Kjaer M. Role of extracellular matrix in adaptation of tendon and skeletal muscle to mechanical loading. *Physiol Rev*. 2004;84(2):649-698. https://doi.org/10.1152/physrev.00031.2003
58. Orr AW, Helmke BP, Blackman BR, Schwartz MA. Mechanisms of mechanotransduction. *Dev Cell*. 2006;10(1):11-20. https://doi.org/10.1016/j.devcel.2005.12.006
59. Smith DA, Carland CR, Guo Y, Bernstein SI. Getting folded: chaperone proteins in muscle development, maintenance and disease. *Anat Rec*. 2014;297(9):1637-1649. https://doi.org/10.1002/ar.22980
60. Ulbricht A, Arndt V, Höhfeld J. Chaperone-assisted proteostasis is essential for mechanotransduction in mammalian cells. *Commun Integr Biol*. 2013;6(4):e24925. https://doi.org/10.4161/cib.24925
61. Tidball JG. Mechanical signal transduction in skeletal muscle growth and adaptation. *J Appl Physiol*. 2005;98(5):1900-1908. https://doi.org/10.1152/japplphysiol.01178.2004
62. Spangenburg EE. Changes in muscle mass with mechanical load: possible cellular mechanisms. *Appl Physiol Nutr Metab*. 2009;34(3):328-335. https://doi.org/10.1139/H09-010
63. Hector AJ, McGlory C, Phillips SM. The influence of mechanical loading on skeletal muscle protein turnover. *Cell Mol Exerc Physiol*. 2015;4(1):1-7. https://doi.org/10.7457/cmep.v4i1.e8
64. Wilkinson DJ, Cegielski J, Phillips BE, et al. Internal comparison between deuterium oxide (D2O) and L-[ring-13C6] phenylalanine for acute measurement of muscle protein synthesis in humans. *Physiol Rep*. 2015;3(7):1-9. https://doi.org/10.14814/phy2.12433
65. Shad BJ, Thompson JL, Holwerda AM, et al. One week of step reduction lowers myofibrillar protein synthesis rates in young men. *Med Sci Sports Exerc*. 2019;51(10):2125-2134. https://doi.org/10.1249/MSS.0000000000002034
66. Catena V, Fanciulli M. Deptor: not only a mTOR inhibitor. *J Exp Clin Cancer Res*. 2017;36(1):12. https://doi.org/10.1186/s13046-016-0484-y
67. Weigl LG. Lost in translation: regulation of skeletal muscle protein synthesis. *Curr Opin Pharmacol*. 2012;12(3):377-382. https://doi.org/10.1016/j.coph.2012.02.017
68. Shimkus KL, Wudeck EV, Shirazi-fard Y, et al. DEPTOR expression correlates with muscle protein synthesis. *Int J Exerc Sci Conf Proc*. 2013;2(5):7.
69. Kazi AA, Hong-Brown L, Lang SM, Lang CH. Deptor knockdown enhances mTOR activity and protein synthesis in myocytes and ameliorates disuse muscle atrophy. *Mol Med*. 2011;17(9-10):925-936. https://doi.org/10.2119/molmed.2011.00070
70. Peterson TR, Laplante M, Thoreen CC, et al. DEPTOR is an mTOR inhibitor frequently overexpressed in multiple myeloma cells and required for their survival. *Cell*. 2009;137(5):873-886. https://doi.org/10.1016/j.cell.2009.03.046
71. Varusai TM, Nguyen LK. Dynamic modelling of the mTOR signalling network reveals complex emergent behaviours conferred by DEPTOR. *Sci Rep*. 2018;8(1):643. https://doi.org/10.1038/s41598-017-18400-z
72. Laplante M, Sabatini DM. mTOR signaling at a glance. *J Cell Sci*. 2009;122(Pt 20):3589-3594. https://doi.org/10.1242/jcs.051011
73. Stelzer G, Rosen N, Plaschkes I, et al. The GeneCards Suite: from gene data mining to disease genome sequence analyses. *Curr Protoc Bioinforma*. 2016;54:1.30.1-1.30.33. https://doi.org/10.1002/cpbi.5
74. Bodine SC, Baehr LM. Skeletal muscle atrophy and the E3 ubiquitin ligases MuRF1 and MAFbx/atrogin-1. *Am J Physiol Endocrinol Metab*. 2014;307(6):E469-E484. https://doi.org/10.1152/ajpendo.00204.2014
75. Suetta C, Frandsen U, Jensen L, et al. Aging affects the transcriptional regulation of human skeletal muscle disuse atrophy. *PLoS ONE*. 2012;7(12):e51238. https://doi.org/10.1371/journal.pone.0051238
76. Chen Y-W, Gregory CM, Scarborough MT, et al. Transcriptional pathways associated with skeletal muscle disuse atrophy in humans. *Physiol Genomics*. 2007;31(3):510-520. https://doi.org/10.1152/physiolgenomics.00115.2006
77. Jones SW, Hill RJ, Krasney PA, et al. Disuse atrophy and exercise rehabilitation in humans profoundly affects the expression of genes associated with the regulation of skeletal muscle mass. *FASEB J*. 2004;18(9):1025-1027. https://doi.org/10.1096/fj.03-1228fje
78. Dirks ML, Wall BT, Snijders T, et al. Neuromuscular electrical stimulation prevents muscle disuse atrophy during leg immobilization in humans. *Acta Physiol*. 2014;210(3):628-641. https://doi.org/10.1111/apha.12200
79. Tesch PA, von Walden F, Gustafsson T, Linnehan RM, Trappe TA. Skeletal muscle proteolysis in response to short-term unloading in humans. *J Appl Physiol*. 2008;105(3):902-906. https://doi.org/10.1152/japplphysiol.90558.2008
80. Ferrando AA, Lane HW, Stuart CA, Davis-Street J, Wolfe RR. Prolonged bed rest decreases skeletal muscle and whole body protein synthesis. *Am J Physiol*. 1996;270(4 Pt 1):E627-E633. https://doi.org/10.1152/ajpendo.1996.270.4.E627
81. Symons TB, Sheffield-Moore M, Chinkes DL, Ferrando AA, Paddon-Jones D. Artificial gravity maintains skeletal muscle protein synthesis during 21 days of simulated microgravity. *J Appl Physiol*. 2009;107(1):34-38. https://doi.org/10.1152/japplphysiol.91137.2008
82. Mahmassani ZS, Reidy PT, McKenzie AI, et al. Age-dependent skeletal muscle transcriptome response to bed rest-induced atrophy. *J Appl Physiol*. 2019;126(4):894-902. https://doi.org/10.1152/japplphysiol.00811.2018
83. Alibegovic AC, Sonne MP, Højbjerre L, et al. Insulin resistance induced by physical inactivity is associated with multiple transcriptional changes in skeletal muscle in young men. *Am J Physiol Endocrinol Metab*. 2010;299(5):E752-E763. https://doi.org/10.1152/ajpendo.00590.2009
84. Mouisel E, Blondet B, Escourrou P, et al. Outcome of acetylcholinesterase deficiency for neuromuscular functioning. *Neurosci Res*. 2006;55(4):389-396. https://doi.org/10.1016/j.neures.2006.05.002
85. Edwards SJ, Smeuninx B, Mckendry J, et al. High-dose leucine supplementation does not prevent muscle atrophy or strength loss over 7 days of immobilization in healthy young males. *Am J Clin Nutr*. 2020;112(5):1368-1381. https://doi.org/10.1093/ajcn/nqaa229
86. Wall BT, Snijders T, Senden JMG, et al. Disuse impairs the muscle protein synthetic response to protein ingestion in healthy men. *J Clin Endocrinol Metab*. 2013;98(12):4872-4881. https://doi.org/10.1210/jc.2013-2098
87. Rakobowchuk M, Crozier J, Glover EI, et al. Short-term unilateral leg immobilization alters peripheral but not central arterial

structure and function in healthy young humans. *Eur J Appl Physiol*. 2011;111(2):203-210. https://doi.org/10.1007/s00421-010-1636-y

88. Clark BC, Manini TM, Ordway NR, Ploutz-Snyder LL. Leg muscle activity during walking with assistive devices at varying levels of weight bearing. *Arch Phys Med Rehabil*. 2004;85(9):1555-1560. https://doi.org/10.1016/j.apmr.2003.09.011
89. Langfelder P, Horvath S. *WGCNA Package FAQ*. 2017. https://horvath.genetics.ucla.edu/html/CoexpressionNetwork/Rpackages/WGCNA/faq.html. Accessed June 25, 2020.
90. Allen JD, Xie Y, Chen M, Girard L, Xiao G. Comparing statistical methods for constructing large scale gene networks. *PLoS ONE*. 2012;7(1):e29348. https://doi.org/10.1371/journal.pone.0029348
91. Li J, Zhou D, Qiu W, et al. Application of weighted gene co-expression network analysis for data from paired design. *Sci Rep*. 2018;8(1):622. https://doi.org/10.1038/s41598-017-18705-z
92. Shannon P, Markiel A, Ozier O, et al. Cytoscape: a software environment for integrated models of biomolecular interaction networks. *Genome Res*. 2003;13(11):2498-2504. https://doi.org/10.1101/gr.1239303

SUPPORTING INFORMATION

Additional Supporting Information may be found online in the Supporting Information section.

How to cite this article: Willis CRG, Gallagher IJ, Wilkinson DJ, et al. Transcriptomic links to muscle mass loss and declines in cumulative muscle protein synthesis during short-term disuse in healthy younger humans. *FASEB J*. 2021;35:e21830. https://doi.org/10.1096/fj.202100276RR